SPE Paper Number 77700

Capillary Shockwave Front Blind Imaging of Reservoir Limits: A Case Study

Fred L. Goldsberry, WAVEX®, Inc. and Kevin C. Anderegg, Devon Energy Corporation

Abstract

Reservoir boundary information is gleaned from a steady-flowrate-drawdown test and/or a subsequent buildup following the steady flow period. Singularities are observed to be present in virtually all transient pressure data that can provide direct information about the limits around a well. Multiple limits can be detected discretely and described by distance from the well and angular shape at the point of contact. The input information required is pressure data acquired while flowing on a fixed choke, petrophysical properties from cores and electric logs, and fluid production rates and compositions during the flow period.[2]

Reservoir limits can be assembled into an energy equivalent image based upon cone of influence energy growth behind a bounding initiating capillary pressure shockwave front. The resulting image can then be compared with a seismic data based map or a geologic map. Volume integrals for gas inplace can provide an early physical measurement for reserve accounting purposes.[4,5,6,8]

A variety of boundary contact shapes were assembled into a “blind” energy map that was later confirmed by seismic imaging. A direct overlay comparison of the “blind” energy image and a 3D seismic map is presented. The limit information will be compared with the seismic image to confirm it point by point.

This new transient pressure analysis method is based upon a real capillary network growing from the well bore. Flow into the well bore is restricted to radial flow and confined to the real capillary flow paths by initial capillary pressure.[2] The cone of influence is bounded by an associated capillary shockwave front that restricts its growth. The bounding initiating capillary pressure shockwave front is the physical phenomenon that exists at the radius of investigation.[1,7,10] The capillary networks give rise to secondary pressure singularities when a boundary is encountered. The method extends traditional analysis to the realm of wave mechanics[8,9,11] and allows direct data processing. The solution is based upon an energy model that solves for boundary geometry directly from flow and buildup data without the process of traditional iterative history matching. The boundary contacts can then be assembled into an image of the reservoir based upon relative disposition of individual limit contact.

The Problem

A single well reservoir had been successfully drilled in the Eugene Island Area and was being produced by Well No. B-13ST. This particular single well reservoir was identified as an attractive testing candidate for the operator because of its multi-faceted structure and questions regarding closure and water drive. The structural trap was composed of numerous splinter faults that held the possibility of discontinuous or leaky connection to another fault block. At issue was whether the reservoir trap was sealing up dip and how large a reserve base was represented by the fault closure. This other fault block would be an ideal candidate for a second well or future sidetrack of the existing well if it was indeed separate. Additionally, the operator was interested in increasing the booked reserves attributed to the well by confirming the reservoir limits indicated by the 3D seismic data.

The Solution

The operator has long owned and utilized a surface mount dual quartz transducer pressure recorder that has provided substantial quantities of data by recording long term initial drawdowns. Data acquisition is simple. Place the well on production on a fixed choke that is designed to produce the well at a moderate rate. This allows the completion to settle in before stressing it fully. This period may be brought to an end with an extended buildup test followed by another drawdown period. The result is that often the limits near the well are seen three times as data singularities and often the entire reservoir is explored during the first drawdown. In this case the initial drawdown was sufficient to define the reservoir boundaries. Figure 1 shows the drawdown data.

The startup was ramped up and held steady on a fixed choke for approximately 80 hours before control problems obscured the data. There are numerous shut-ins and some small rate changes that are associated with start up. The data in Figure 1 appear to be non-descript until replotted on a semi-log plot in Figure 2.

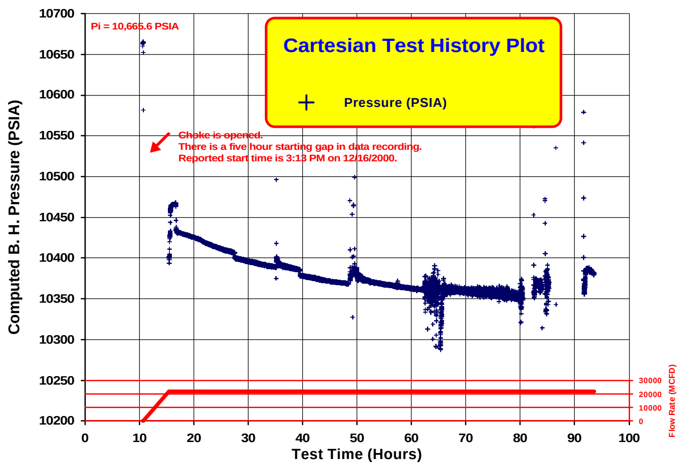

Figure 1. Cartesian Plot of Test History

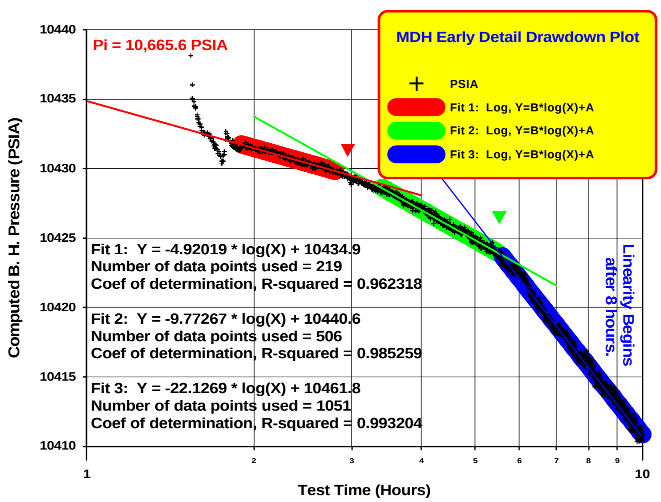

Figure 2. Semi-Log Plot of Drawdown Mid-Time and Late Region

Note that the expanded scale of Figure 2 reveals three straight-line sections. The sections are established as statistical fits of the data (natural log of time vs. pressure). The straight nature of the data over sections of the plot is the result of the response of a well under control of a fixed choke and the interaction of capillary flow paths encountering a reservoir limit. The slope increase is the response of the well to the failure of the cone to grow beyond the limit. This produces a natural reduction in the flow to the well, which results in an increase of drawdown to make up the difference in flow. The result is an immediate response to a limit that perpetuates with the test or until another limit is encountered. Figure 3 describes the capillary structure of the cone of influence during the drawdown when a limit is encountered. Each limit contact results in its own secondary cone of influence. The secondary boundaries are separated from each other by secondary capillary shockwave fronts that grow in proportional speed to the outer shockwave front. The outer shockwave front exists at the radius of investigation and functions as the boundary condition of the cone of influence.

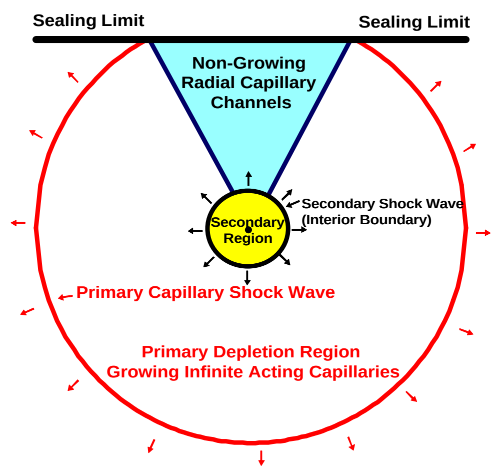

Figure 3. Cone of Influence Schematic Striking a Straight Limit

The fan of capillaries that has stopped growing represents a collection of fixed volume capillaries. All other capillaries continue to grow as though the reservoir was infinitely large. In times past, the mid-time region was described as infinite acting radial flow. The characteristic non-diffusive behavior has been recognized in transient well test data since the inception of well testing. Diffusion theory does not predict this behavior. Mirror image well theory was popularized in the 1950's but failed to provide an explanation for these observations. Widespread use of these singularities was in vogue until the advent of digital reservoir simulation. There have been numerous attempts over the years to use reflected waves and wave equivalents without the attendant physical explanation of why these occur or for that matter what they are. The scope of this paper is not intended to provide a full physical explanation but to provide a practical example of what may be accomplished. The solution method(2) is referenced for those interested in the physical theory and method. The semi-log slope is proportional to the energy decay rate in the section of the cone of influence being observed by the pressure gauge.

Further examination of the data at later times revealed a small energy shift and a final limit as detailed in Figures 4 and 5.

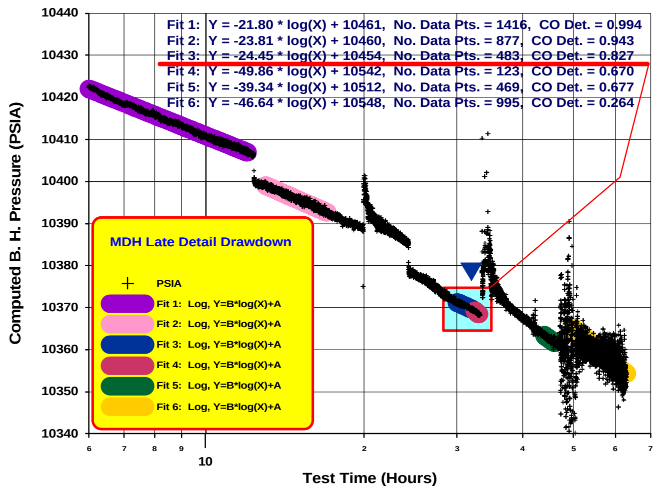

Figure 4. Limit 3 Position from Energy Shift

Note the limit shift marked by a blue triangle. The energy decay or slope calculation is approximately 22-24 psi/ln cycle before this point and consistently 39-49 psi/ln cycle thereafter. The energy shift must occur before 40 hours and after 30 hours. The best pick for the time at which this occurs is at approximately 32.8 hours as can be seen on Figure 5.

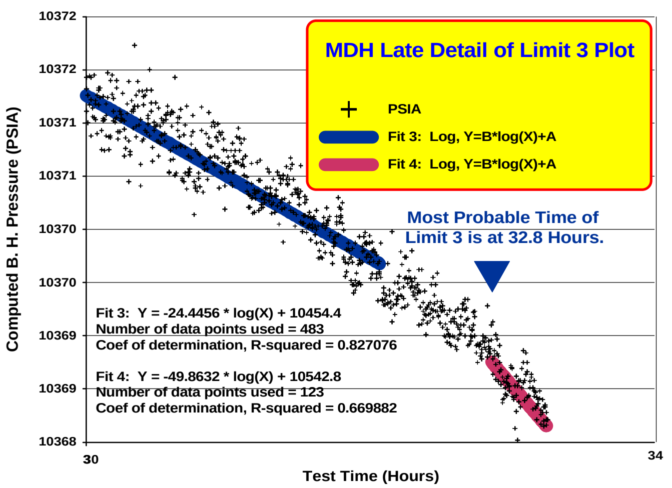

Figure 5. Limit 3 Detail

Each of these major limit events is input to the nested cone energy model. For each energy shift a characteristic shape at the point of contact is calculated. The time provides the radius of the capillary shockwave front from the well. The result is a limit diagram as shown in Figure 6. The energy growth is depicted in a polar plot that is shown in yellow.

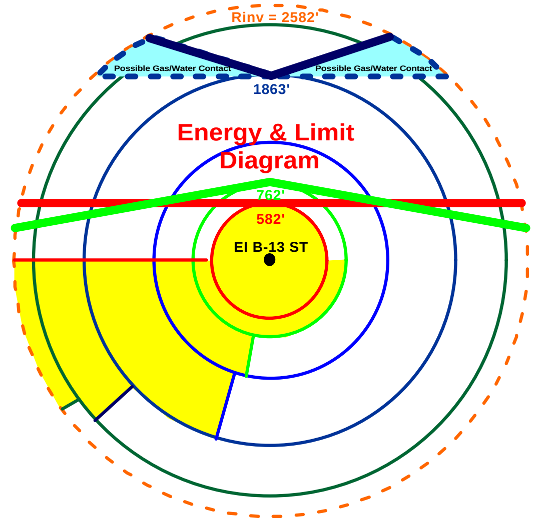

Figure 6. Limit and Energy Diagram

The limits are placed in a single direction from the well. This is because we do not know the direction and must arbitrarily assign a position to the first limit. The other limits will be placed relative to limit 1 around the energy diagram. The energy diagram is laid out to show the calculated angles of splay.

The options for relative limit position are several. The fact that a wedge of capillaries striking the limit defines each limit restricts the number of positions in which a limit may be placed. The relative relationships are 1-2-3-4 or 1-3-2-4 or 1-2-4-3. Once limit placements are made, a series of energy calculations are made to determine which configuration represents the best energy balance for the system through the end of the test. In this case the radius of investigation is boundary 4. In Figure 7 we begin with the placement of limits in a 1-2-3-4 rotation.

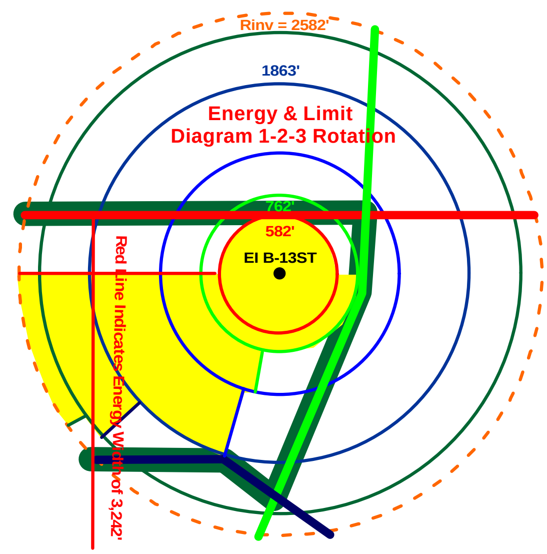

Figure 7. Limits Placed Around the Energy Diagram

Note that the linearity of the data as seen in Figure 8 suggests growth between parallel limits and then a splay in the system at about 50 hours. More importantly it suggests that the 1-2-3-4 limit rotation may not be the best choice.

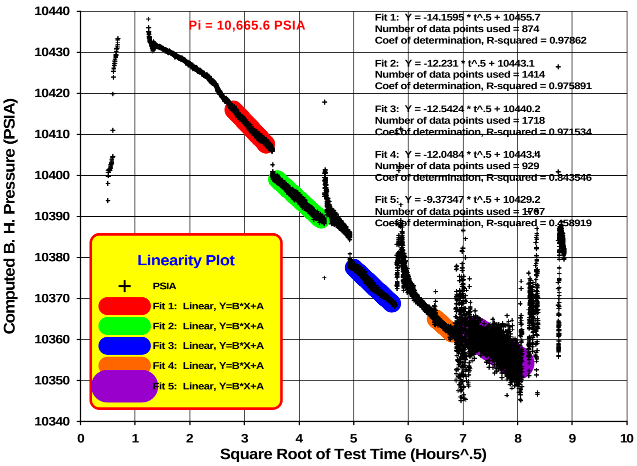

Figure 8. Linearity Plot

Now it is necessary to construct trial 2 around an energy diagram. Note that the energy diagram of Figure 9 can be split to provide another case, which involves limits 1 and 2 being opposites. Again, the limit width calculations at extended test time suggest a misfit on width calculations. Further, the projection of limit 2 in green is inconsistent with the energy diagram.

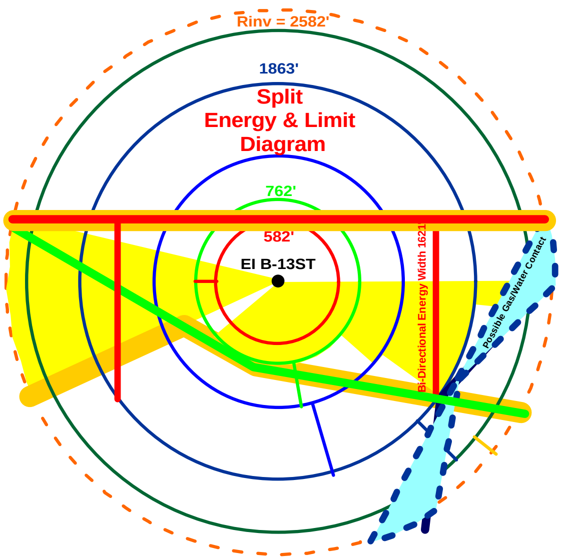

Figure 9. Limit 1 Opposite Limit 2 Bi-Directional Growth of the Cone of Influence

The next construction, in Figure 10, shows limits rotated in a 2-1-3 sequence around the energy diagram. Each image is displayed on a transparency and may be flipped over to see the mirror image. The mirror image or flip side is just as valid as the first. This method is indifferent to direction and is reflective only of the relative direction. This time the linearity calculation is used to fit limit 3 relative to limits 1 & 2 in order to produce the appropriate energy growth splay at the end of the test.

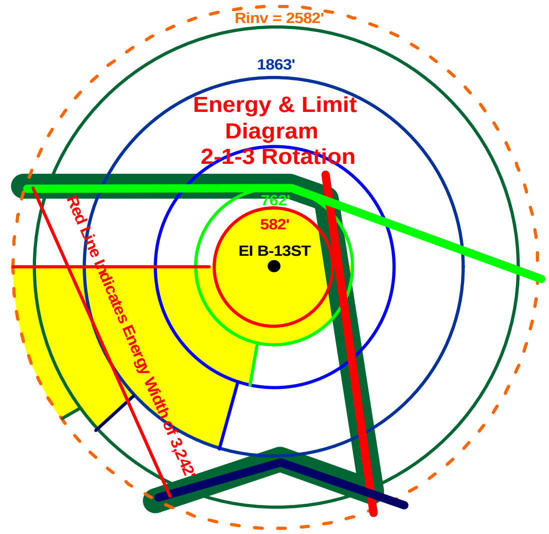

Figure 10. Final Relative Limit Configuration Case

Up to this point, it has not been necessary to refer to a geologic map. Inputs included pay count from an electric log and cores, fluid production rates and compositions, and finally high resolution and stability pressure data. The solution is the result of a proprietary nested cone radial capillary energy model(2). This is accomplished from observing elastic energy growth. Figure 10 is a Blind Energy Image and Figure 11 is the Geologic/Geophysical Map.

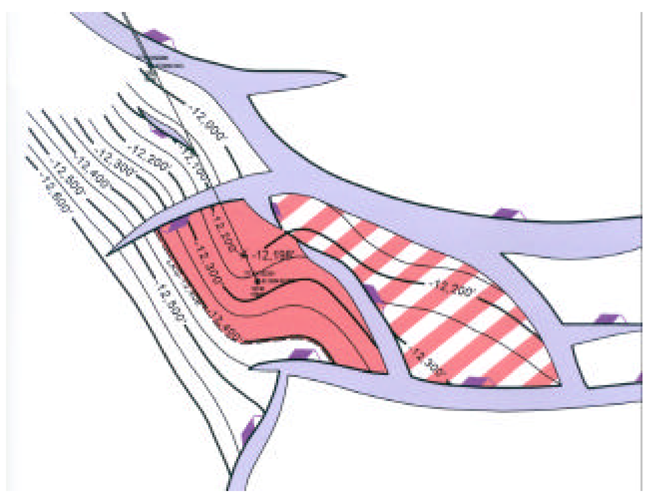

Figure 11. Geologic/Geophysical Map

The energy map is solely the result of the energy balance within and expanding cone of influence. The growth of the system is restricted by the initiating capillary pressure of each pore throat. The cone of influence is bounded by a moving wall of capillary breakdown pressure. This is a geophysical process independent of the traditional seismic measurement. Seismic images are produced soundwaves from the top down. Energy maps are produced by the radial growth of a shockwave front emanating from the wellbore. When two independent measurements produce images that bear many points of volumetric, angular, and dimensional similarity, there is a high probability that the maps are correct. This independence also suggests that the data acquisition and deconvolution of soundwaves and pressure singularities was accurate. Otherwise one must assume the geophysicist, the petrophysicist, and the pressure analyst have made equal and offsetting errors in their respective models and data processing.

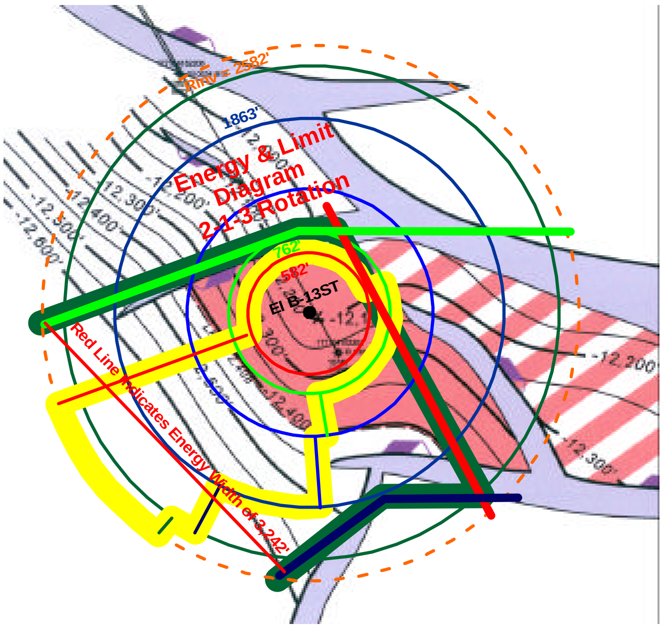

Figure 12. Map and Energy Image Overlay

Note the twelve points of comformance below and consider the ***value added*** to the certainty of the geologic picture.

1. **Distance to Limit 1**
2. **Shape of Limit 1**
3. **Distance to Limit 2**
4. **Shape of Limit 2**
5. **Distance to Limit 3**
6. **Shape of Limit 3**
7. **Corner of Limits 1 & 3**
8. **Corner of Limits 1 & 2**
9. **Response to the Spur Fault of Limit 3**
10. **Width of Reservoir at End of Test**
11. **Angle of Splay of Reservoir**
12. **Integral Volume for Gas Inplace**

Performance Confirms Results

The operator's two main objectives for the well test were to confirm the reservoir limits indicated by the 3D seismic data and to increase the proven reserves attributed to the well. The first limit indicated that the possible leaking fault to the east of the wellbore was sealing, leaving a separate fault block to the east as shown in Figure 12. Based on indications that the sand is thinning to the east, the separate fault block will be developed by a sidetrack of the B-13ST once it depletes.

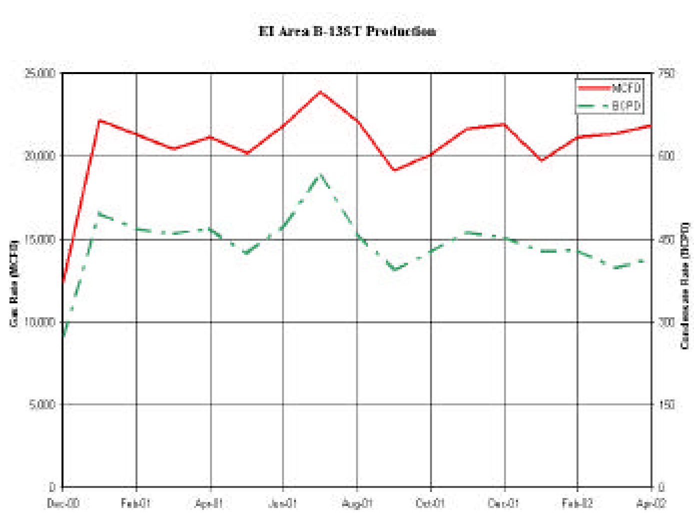

Figure 13. EI Area B-13ST Production History

Initial proven reserves in the B-13ST were based on a lowest known gas in the well. Based on geology and geophysics, a value for gas in place was computed based on the gas-water contact indicated from the 3D seismic survey. The integral volume for gas-in-place calculated from the test data agreed closely with the gas in place calculated using the geologic/geophysical data. ***Confirmation of the reservoir volume by energy imaging led to an increase in third party recognized proven recoverable reserves of 175%!***

To date the B-13ST has produced 11 BCF and 240 MBC. This represents 40 to 45% of the gas-in-place. Production has averaged 22 MMCFD and 450 BCPD for the life of the well as shown in Figure 13***. A subsequent material balance study of the reservoir has confirmed the initial gas-in-place estimates.*** Table 1 lists each of the estimates for gas-in-place calculated for the reservoir along with the time from the date of first production required to arrive at the estimate.

Testing not only confirms seismic but also provides an early confirmation of reserves. ***When energy imaging is used as a blind crosscheck with seismic imaging, confidence levels are improved.*** Transient energy based volumetric dimensioning supports the operator's early economic decisions on the well and the property. Energy imaging can be used as a complement or a cost-effective alternative to tracking gas/ water contacts.[(3)]

Method of Calculation	Time to Estimate (From date of first production)	OGIP Estimate (BCF)
Volumetric Using Geology/Geophysics	0 Days	24.6
Pressure Transient Analysis	10 Days	27.2
Material Balance	16 Months	23.6

Table 1. Timing of Reserves Information

Prospects are drilled from seismic data. Seismic methods can be used to estimate volume when used in conjuction with formation evaluation and velocity electric logs that are available only after drilling. At this point the operator has a volumetric estimate based upon sound wave reflection.

After the discovery well is drilled, flow testing provides an energy growth picture by utilizing the integration of elastic energy as the cone of influence is formed and expands to encounter all of the boundaries of the reservoir. By using a ***bounding initiating capillary pressure shockwave model*** and its compliment of ***real radial capillary pathways***, it is possible to produce a second independent image and a reservoir volume at the outset of production. Traditional methods require a much longer pressure history to provide the same information. Pressure testing and shockwave front analysis is a faster way to achieve corroborating results.

The timing of recognition of reserves is important to most operators. Accounting practices require recognition of development costs as part of DD&A. Full reserves recognition including downdip gas typically lags development by as much as three to four years. Probablistic methods have been used to account for this lag. Well testing can be used to confirm 3D seismic based geologic maps allowing third-party engineers to accelerate deterministic SEC reserves by recognizing a “blind” energy test interpretation as other engineering information.

Conclusion

The cone of influence is composed of a radiating capillary structure that responds to each major limit with a shift in decay energy. Figure 14 illustrates the pressure derivative singularities in a buildup followed by an interference cone of influence from an offset well. These are typical of limit responses.

For a relatively small investment in wellhead instrumentation and several days of analysis, it was possible to resolve several reservoir issues within a few days of startup rather waiting for production plots to mature over months and years. It was possible to resolve a geologic question using transient material balances integral to the shockwave front method rather than having to wait for substantial reservoir depletion to occur. ***The test is simple to execute. Install a dual quartz pressure gauge, flow the well on a fixed choke, and sell hydrocarbons.***

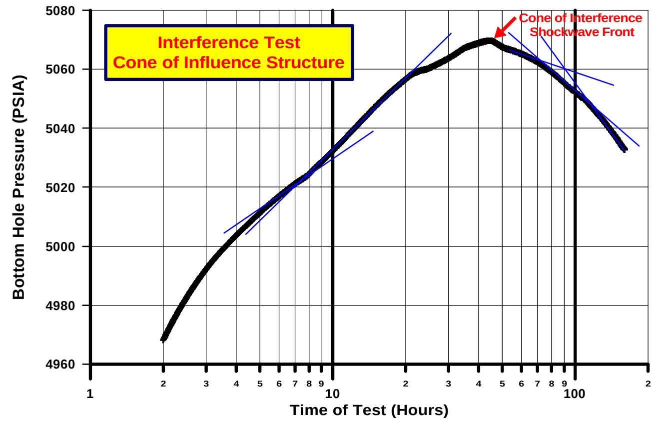

Figure 14. Data Singularities in an Interference Test

An early analysis for limits may impact future well interventions, add drilling locations, or in the case of a DST on a discovery, prevent setting a platform on an uneconomic reservoir. The more expensive the development of well locations, the more important testing can be to the operator’s bottom line. ***Accelerating the booking of reserves is just a part of using well testing to produce confirmation of reservoir volumes and dimensions or calibration of seismic images.***

References

1. Goldsberry, F. L., "Reservoir Conformance Developments – Capillary Shockwaves in Porous Media", 1998-*Fourth International Conference on Reservoir Conformance*, Houston, Aug. 1998.
2. Goldsberry, F. L., "Method for Producing Images of Reservoir Boundaries," U.S. Patent No. 6,041,017, U.S. Patent Journal, U. S. Patent Office, Washington D.C., Mar. 2000.
3. Goldsberry, F. L., Holland, J. T., Gross, W. E., Salzman, D. L., and Wildenstein, R. C., SPE 71456 “Reservoir Conformance: Tracking Gas/Water Contacts via Capillary Shockwave Fronts,” ATCE 2001, New Orleans, Oct. 2001.
4. Hurst W., Clark, J. D., and Brauer, E. B., "The Skin Effect in Producing Wells", 42nd Annual Fall Meeting, SPE of AIME, Houston, Oct. 1967.
5. Hurst, W., Haynie, O. K., and Walker, R. N., "SPE 145 Some Problems in Pressure Buildup", SPE of AIME, Dallas, Oct. 1961.
6. Hurst, W., “Unsteady Flow of Fluids in Oil Reservoirs,” Physics 5, January 1934.
7. Hurst, W., "SPE 2461 – Radius of Drainage Formula - A Technical Note", SPE of AIME, Nov. 1968.
8. Jones, Park J., “Drawdown Exploration Reservoir Limit, Well and Formation Evaluation” Technical Paper No. 824-G AIME, April 1957.
9. Jones, Park J., "Reservoir Limit Tests on Gas Wells", *SPE Gas Technology Symposium*, Tyler, Texas, July 17, 1961, p. 219.
10. Matthews, C. S. and Russell, D. G., "Pressure Buildup and Flow Tests in Wells", Henry L. Doherty Series Monograph Volume 1, SPE of AIME, New York, 1967, pp.87, 94-95.
11. Rowan, G., "SPE 918-G Wave Theory and Free Surfaces…A study of the Motion of Oil Reservoir Fluids", SPE of AIME, Oct. 1957.